

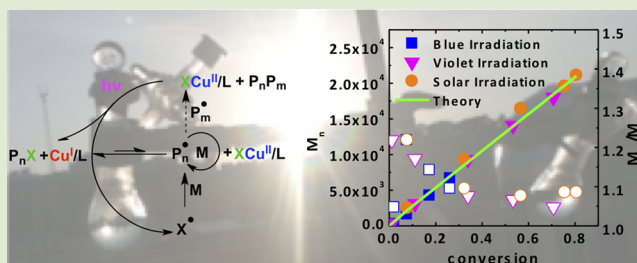
Visible Light and Sunlight Photoinduced ATRP with ppm of Cu Catalyst

Dominik Konkolewicz, Kristin Schröder, Johannes Buback, Stefan Bernhard, and Krzysztof Matyjaszewski*

Department of Chemistry, Carnegie Mellon University, 4400 Fifth Avenue, Pittsburgh, Pennsylvania 15213, United States

S Supporting Information

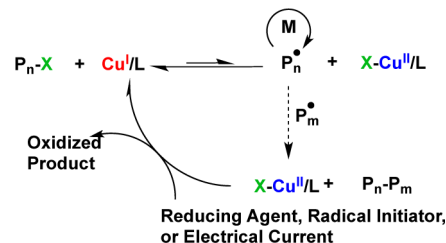
ABSTRACT: Photochemically induced ATRP was performed with visible light and sunlight in the presence of parts per million (ppm) copper catalysts. Illumination of the reaction mixture yielded polymerization in case of 392 and 450 nm light but not for 631 nm light. Sunlight was also a viable source for the photoinduced ATRP. Control experiments suggest photoreduction of the Cu^{II} complex (ligand to metal charge transfer in the excited state), yielding a Cu^{I} complex, and a bromine radical that can initiate polymerization. No photoactivation of Cu^{I} complex was detected. This implies that the mechanism of ATRP in the presence of light is a hybrid of ICAR and ARGET ATRP. The method was also used to synthesize block copolymers and polymerizations in water.



Reversible deactivation radical polymerization (RDRP) has revolutionized the fields of polymer chemistry and material science, because it offers control over the molecular weight and architecture of a polymer similar to anionic living polymerization, with tolerance to functional groups and reaction conditions similar to conventional radical polymerization.¹ Atom transfer radical polymerization (ATRP) is one of the most versatile RDRP methods.² ATRP uses a transition metal catalyst, most commonly a copper catalyst, in a low oxidation state to activate an alkyl halide and generate a radical and the catalyst in a higher oxidation state.³ This radical can add monomer, before being deactivated to the alkyl halide by the catalyst in the higher oxidation state. ATRP has been used to make complex polymeric architectures,⁴ and in materials or biological applications.⁵ One limitation of normal ATRP is the high catalyst loadings needed to maintain a reasonable reaction rate. Recently, methods have been developed that allow parts per million (ppm) concentrations of catalyst to be used in ATRP by continuously regenerating Cu^{I} activators.⁶ These methods include initiators for continuous activator regeneration (ICAR) ATRP,⁷ activators regenerated by electron transfer (ARGET) ATRP,⁸ supplemental activators and reducing agent (SARA) ATRP,⁹ and electrochemically mediated ATRP (eATRP).¹⁰ This is shown in Scheme 1.

It is also interesting to explore the possibility of photoinduced reduction of Cu^{II} halide complexes. The change in oxidation and reduction potentials due to charge transfer in an excited state may allow photoinduced redox processes that are inaccessible from the ground state. The microscopic control of these photochemical reactions, due to the simple triggering by light, is an attractive feature for building molecular architectures. Photoactive catalysts can be tuned to match emission spectra and electrochemical potentials in complex photocatalytic systems. Substantial efforts in this field are

Scheme 1. ATRP with Low Catalyst Loadings



currently directed at the development of solar fuels¹¹ and also novel organic reactions driven by photons.¹² Such redox reactions may be highly efficient, especially if the excited system undergoes stabilization via homogeneous bond dissociation, which could be used for ATRP.

In the initial studies of ATRP in the presence of light, an acceleration in the rate of methyl methacrylate (MMA) was observed using 2,2-dichloroacetophenone as initiator and $\text{CuCl}/2,2'$ -bipyridine as catalyst.¹³ More recently, Cu-mediated ATRP was successfully carried out with various radiation sources with or without various photoinitiators.¹⁴ The photoreduction of the $\text{X-Cu}^{\text{II}}/\text{L}$ deactivator complex to the $\text{Cu}^{\text{I}}/\text{L}$ activator complex in the presence of methanol was reported.^{14a} Very recently, ppm concentrations of Cu and Ir catalysts were used to polymerize methyl methacrylate (MMA) in the absence of photoinitiators.¹⁵ The Ir-based system also polymerized methacrylic acid and benzyl methacrylate.^{15a}

Received: September 1, 2012

Accepted: September 27, 2012

Published: October 4, 2012

Herein, we report the first photoinduced ATRP of both acrylic and methacrylic monomers without photoinitiators and with ppm amounts of Cu catalysts. The mechanism of the photoinduced ATRP was studied using narrow bandwidth light emitting diodes (LEDs). This avoids complications due to absorption at two or more different wavelengths. In addition, the photoinduced ATRP was used to make block copolymers, and the reaction was performed in water.

In the past, either high copper concentrations, photoinitiators, or UV sources (with multiple emission wavelengths) were used. This work uses low copper concentrations and mild light sources: sunlight and light emitting diodes with narrow emission ranges. Three LEDs were employed, emitting in the violet (392 ± 7 nm), blue (450 ± 10 nm), or red spectral region (631 ± 9 nm), as shown in Figure S1.¹⁶ The intensities of the photoreactors were found to be 0.90 ± 0.05 , 10.0 ± 0.5 , and 8.9 ± 0.5 mW/cm² for the violet, blue, and red photoreactors, respectively. Methyl methacrylate (MMA), oligo(ethylene oxide) monomethyl ether methacrylate (molecular weight 300; OEOMA), ethyl acrylate (EA), and methyl acrylate (MA) were used as monomers. As ATRP initiators, ethyl α -bromoisobutyrate (EBiB) was used for acrylates and ethyl α -bromophenylacetate (EBPA) for methacrylates. As ATRP catalysts, CuBr₂ complexes with tris(2-pyridylmethyl) amine (TPMA), *N,N,N',N'',N'''*-pentamethyldiethylenetriamine (PMDETA), and tris((4-methoxy-3,5-dimethylpyridin-2-yl)methyl)amine (TPMA*) were used. The latter complex is the most active ATRP catalysts and suitable for the polymerization of acrylates.¹⁷ When organic solvents, like DMF, were used, a ratio of Cu to ligand of 1:4.5 was chosen to ensure efficient complexation at low catalyst loadings, following literature.¹⁷ Figure S2 shows the UV/vis/NIR spectra of CuBr₂/TPMA in MMA/DMF and CuBr₂/TPMA* in MA/DMF. The spectra are similar and show that the extinction coefficient at the blue LED emission peak (450 nm) is similar to that at the red LED emission peak (631 nm) and about 20 times smaller than at the violet LED emission peak (392 nm).

Figure 1 shows typical results of polymerization of MA in 50% DMF at room temperature with 100 ppm of CuBr₂ and TPMA* ligand for a targeted degree of polymerization of DP = 300. Upon irradiation, polymerization started after a short induction period and was fastest with sunlight, slower with violet irradiation and even slower with blue irradiation, and it did not occur with red irradiation. In all cases, control of polymerization was excellent, molecular weights agreed with the theoretical values and M_w/M_n reached values below 1.1.

The correlation of the rate with the irradiation wavelength can be explained by the UV/vis spectra (Figure S2). The Cu^{II} complexes absorb very strongly in the UV, with significant absorption in the violet, and weaker absorption in the blue region. Because the solar spectrum extends into the UV, the polymerization is faster than with violet or blue irradiation. Although the absorbance is 20 times higher at 392 nm, than 450 nm, the intensity of the violet LEDs is 10 times lower. Therefore, the reaction is about 1.5–2 times faster at 392 nm than at 450 nm. The intensity of blue and red LEDs are similar and extinction coefficients at 631 and 450 nm are similar. However, no polymerization upon irradiation at 631 nm suggests that an efficient ligand to metal charge transfer (LMCT) in the excited state is needed, which does not occur at 631 nm.¹⁸ More detailed studies of photoinduced polymerization of MMA and MA at different wavelengths (λ) and variable conditions are presented in Tables 1 and 2, and the

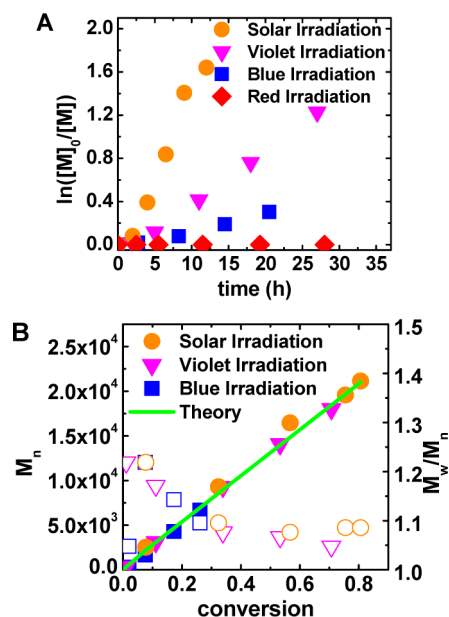


Figure 1. (A) Kinetics and (B) M_n (solid points) and M_w/M_n (open points) evolution in polymerization of MA using different radiation sources. Conditions: $[MA]/[EBiB]/[CuBr_2]/[TPMA^*] = 300:1:0.03:0.135$ in 50 vol% DMF at room temperature (r.t.).

kinetics of polymerization for the 392, 450, and 631 nm irradiation are shown in Figure S3 for the MMA system and Figure S4 for the MA system. For both systems there is an increase in the reaction rate when the shorter irradiation wavelengths are used, Tables 1 and 2 (entries 1–3). The Supporting Information shows that there is minimal heating during the reaction.

To better understand the effect of light on ATRP, the effect of the different components in the polymerization was investigated. Blank experiments with either monomer only, monomer and initiator only, or monomer and catalyst only were performed for MMA (Table 1, entries 4–6) and for MA (Table 2, entries 4–6). The UV/vis/NIR spectra of these solutions are given in Figure S5, showing that the majority of the absorbance comes from the Cu complex. For MMA, there is a small extent of photoinduced polymerization in the pure monomer after 28 h, but this is only about 3%, compared to 60%, in the presence of catalyst and initiator. Irradiation of MMA with EBPA as initiator alone results in some polymerization, most likely due to photoinduced radicals from this very active initiator.¹⁹ In contrast, for the MA and MA plus EBiB systems, no detectable polymerization occurred, even after 27.5 h. When the monomer and catalyst mixtures were exposed to 392 nm radiation, the polymerization proceeded both for the MMA and the MA systems (Table 1, entry 6 for MMA, and Table 2, entry 6 for MA). In both cases the rate was smaller than for the monomer/initiator/catalyst system. Interestingly, the molecular weight evolution with conversion was similar for both the MMA with catalyst and MA with catalyst. The molecular weights were very large and grew with conversion, although in a nonlinear fashion (Figures S6 and S7).

Another factor to consider was the effect of Cu/ligand complex activity on the polymerization. Table 1 (entries 1 and 7) and Table 2 (entries 1 and 7) show the effect of using a less active catalyst based on PMDETA for MMA and unsubstituted TPMA for MA.¹⁹ Polymerization of MMA with CuBr₂/PMDETA was slightly slower, but polymers had significantly

Table 1. Photoinduced ATRP of Methyl Methacrylate (MMA)

entry ^a	[M]/[I]	λ (nm)	cat. loading (ppm)	catalyst	t (h)	conv.	$M_{n, \text{GPC}}$	$M_{n, \text{theo}}$	M_w/M_n
1	300:1	392	100	TPMA	27	0.58	18000	17600	1.09
2	300:1	450	100	TPMA	20.5	0.28	10000	8700	1.08
3	300:1	631	100	TPMA	28	0			
4	300:0	392	0		28	0.03	200000		2.7
5	300:1	392	0		28	0.23	270000	7230	2.1
6	300:0	392	100	TPMA	28	0.29	610000		2.2
7	300:1	392	100	PMDETA	28	0.52	17000	15900	1.19
8 ^{b,c}	300:1	Sun	100	TPMA	32	0.82	25000	24900	1.13
9 ^d	300:1	392	100	TPMA	27	0.47	15000	14300	1.10

^aPhotoinduced ATRP conditions: [MMA]/[EBPA]/[CuBr₂]/[L] = 300:1:0.03:0.135 with 50 vol % DMF at room temperature (23 °C). ^b14 h dark period between 12 and 26 h. ^cMaximum temperature 29 °C on first day; 33 °C on second day. ^dTemperature, 29 °C.

Table 2. Photoinduced ATRP of Methyl Acrylate (MA)

entry ^a	[M]/[I]	λ (nm)	cat. loading (ppm)	catalyst	t (h)	conv.	$M_{n, \text{GPC}}$	$M_{n, \text{theo}}$	M_w/M_n
1	300:1	392	100	TPMA*	27	0.71	18000	18500	1.05
2	300:1	450	100	TPMA*	20.5	0.26	6700	7300	1.10
3	300:1	631	100	TPMA*	28	0			
4	300:0	392	0		27.5	0			
5	300:1	392	0		27.5	0			
6	300:0	392	100	TPMA*	27.5	0.14	150000		1.6
7	300:1	392	100	TPMA	28	0.45	12000	11800	1.07
8 ^b	300:1	Sun	100	TPMA*	12	0.81	21000	21000	1.09

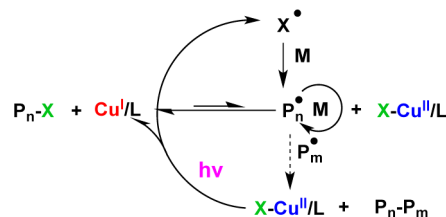
^aPhotoinduced ATRP conditions: [MA]/[EBiB]/[CuBr₂]/[L] = 300:1:0.03:0.135 with 50 vol % DMF at room temperature (23 °C). ^bMaximum temperature, 29 °C.

higher M_w/M_n . For MA with CuBr₂/TPMA polymerization was much slower than with CuBr₂/TPMA*, but M_w/M_n values were similar. The UV/vis spectra are shown in Figure S8 for the MMA with CuBr₂/PMDETA system and Figure S9 for the MA with CuBr₂/TPMA. The kinetics of the MMA with CuBr₂/PMDETA and CuBr₂/TPMA systems are compared in Figure S10, and the kinetics of the MA with CuBr₂/TPMA and CuBr₂/TPMA* system are compared in Figure S11.

Photon-driven redox chemistry is common for Cu^{II} polypyridine complexes.^{18,20} These complexes exhibit weak d–d transitions in the red and the near-IR as well as a very strong absorption in the UV that is generally assigned to a ligand to metal transition (Figure S2). A completely transparent region between 500 and 600 nm is very characteristic for all the studied copper complexes. This feature explains the unexpected and unusual observation that a photopolymerization is possible from a high-energy excited state and that the chromophore is not instantly deactivated to the ground state via internal conversion. The photoirradiation can induce a redox reaction of CuBr₂/L deactivator complex to CuBr/L activator plus bromine radical to start the polymerization and then continue to regenerate the activator lost in the biradical termination process, as in ARGET or ICAR ATRP. A second possible process may be the photoactivation of the lower oxidation state transition metal complex, as proposed for Ir and also for Cu-based systems.¹⁵ However, the directly measured activation rate coefficient in the presence of 392 nm radiation showed no appreciable difference with the one measured in dark (Figure S12). Thus, the results reported in this paper are best explained by the photoreduction of the X-Cu^{II}/L deactivator complex to give Cu^I/L and a halogen radical. This process has been proposed for various Cu^{II} halide complexes.^{14a,18,20} The halogen radical can react with monomer and initiate growth of a polymeric radical that is subject to the ATRP equilibrium.

When an alkyl halide is added, these new chains represent a very small fraction of all chains, assuring a good control over the molecular weight (like in ICAR ATRP). In the absence of alkyl halide, chains can only be generated by photoreduction. This implies that as the reaction progresses there will be some chains formed early in the reaction which have a high molecular weight, but also some formed later in the reaction with, consequently, lower molecular weights. This explains the molecular weight evolution illustrated in Figures S6 and S7.

The proposed mechanism for photoinduced ATRP is shown in Scheme 2. This mechanism is a hybrid of ICAR ATRP and

Scheme 2. Mechanism of Photoinduced ATRP

ARGET ATRP. Because the radiation induces the reduction of X-Cu^{II}/L to Cu^I/L, the mechanism resembles ARGET ATRP. However, a halogen radical is formed, which resembles the generation of radicals in ICAR ATRP.

Because the photoinduced ATRP system only requires photons to drive the reaction forward, any light source with sufficiently energetic photons could be used. Therefore, sunlight was used to drive the reaction in Tables 1 and 2 (entry 8). The reactions with sunlight are shown in Figure 1 for polymerization of MA and Figure S13 for MMA, both showing rapid polymerization and good control. The maximum temperature of the day was 29 °C, and an average temperature

difference of 3 °C between sunlight and shade was observed. To determine the effect of temperature, a reaction at 29 °C was irradiated by violet light (Table 1, entry 9), to approximate the average temperature for the sunlight reaction. The polymerization rate was similar at 23 and 29 °C, and the difference was due to a small loss of photons intensity at 29 °C, due to reflections off the water bath, whereas no water bath was used for room temperature reactions. These results suggest that temperatures in the range of 23 to 29 °C have minimal impact on the polymerization and that the increased rate with sunlight is due to the higher intensity of sunlight compared to the LEDs rather than the temperature.

One of the key advantages of ATRP over conventional radical polymerization is its ability to make block copolymers. To confirm block copolymer formation, a PMMA macroinitiator was first prepared by photoinduced ATRP during 23 h, under the conditions given in Table 1 entry 1. This macroinitiator was isolated and chain extended with ethyl acrylate (EA) under conditions analogous to Table 2 entry 1, except that EA was used instead of MA. The UV/vis spectra are shown in Figure S9. Figure 2, illustrates an efficient chain extension of the macroinitiator and formation of a block copolymer.

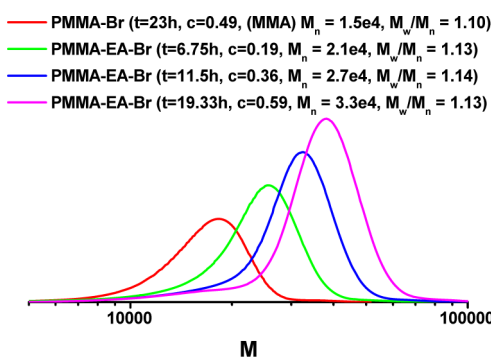


Figure 2. Chain extension of PMMA-Br macroinitiator with EA. Conditions for MMA macroinitiator: $[MMA]/[EBPA]/[CuBr_2]/[TPMA] = 300:1:0.03:0.135$ in 50 vol % DMF. Chain extension conditions: $[EA]/[PMMA-Br]/[CuBr_2]/[TPMA] = 300:1:0.03:0.135$ in 50 vol % DMF. Both reactions are done at room temperature with 392 nm light.

Another advantage of ATRP induced by external stimuli is the possibility of stopping and starting the reaction simply by turning on or off the source, like in eATRP.¹⁰ Figure 3 shows that, in ATRP of MA with $CuBr_2/TPMA^*$ system, the reaction only proceeds while the LED irradiation occurs, and there is essentially no polymerization in the absence of light. Furthermore, the control over the polymerization is excellent, with low M_w/M_n values and good correlation between experimental and theoretical molecular weights. Similar results are seen for the MMA $CuBr_2/TPMA$ system when light is turned on or off (Figure 3).

Finally, to reduce the environmental impact of the photoinduced ATRP process, the reaction was implemented in water as the solvent, to avoid the use of organic solvents.²¹ In water, a ratio of Cu to ligand of 1 to 8 was used to ensure efficient complexation at low catalyst loadings following the literature.^{21b} OEOMA was polymerized in water using a poly(ethylene oxide) monomethyl ether bromoisobutyrate initiator of molecular weight 2000 (PEO-iBBR), 100 ppm of a $CuBr_2/TPMA$ catalyst, with 30 mM NaBr in water (67% by

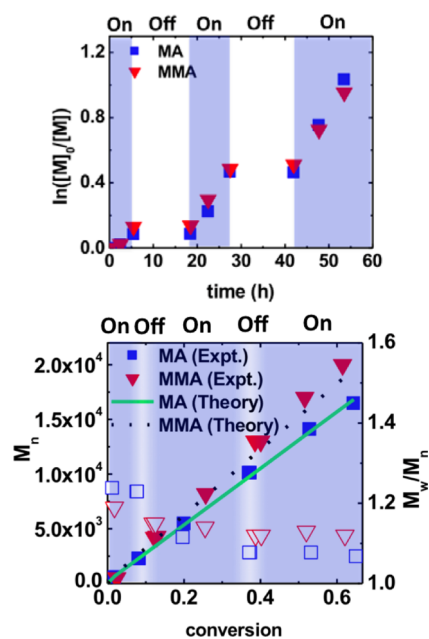


Figure 3. (A) Kinetics and (B) M_n (solid points) and M_w/M_n (open points) for the polymerization of MMA and MA with dark and light (off and on) periods. Conditions: $[MA]/[EBiB]/[CuBr_2]/[TPMA^*] = 300:1:0.03:0.135$ or $[MMA]/[EBPA]/[CuBr_2]/[TPMA] = 300:1:0.03:0.135$, 50 vol % DMF, at room temperature with 392 nm radiation.

volume). The UV/vis spectrum is shown in Figure S8. The results are summarized in Figure S14 and show that the molecular weight grows with conversion, achieving a $M_n = 65000$ and a $M_w/M_n = 1.34$ at 60% conversion after 11.5 h.

In conclusion, photoinduced ATRP of acrylates and methacrylates can be performed at catalyst loadings as low as 100 ppm using mild light sources such as blue or violet LEDs or even sunlight. The control over both acrylic and methacrylic monomers is excellent, and the resulting polymer can be chain extended to a block copolymer. The reaction is consistent with a mechanism where the $X-Cu^{II}/L$ complex undergoes homolytic cleavage in the excited state to generate the Cu^I/L activator complex and a halogen radical, which initiates polymerization. This is expected to occur whenever radiation sources are present, and the interplay of photoinduced reduction and other reduction mechanisms will be the subject of further investigation. One advantage of the photoinduced ATRP, compared to classical ARGET systems, is that the reaction can be ceased and recommenced simply by switching on or off the radiation source. The photoinduced ATRP used in this report is environmentally benign due to the low catalyst concentrations and mild radiation sources, and this work showed that the photoinduced ATRP can be extended to aqueous systems.

■ ASSOCIATED CONTENT

📄 Supporting Information

Experimental details and additional characterization data. This material is available free of charge via the Internet at <http://pubs.acs.org>.

■ AUTHOR INFORMATION

Corresponding Author

*E-mail: km3b@andrew.cmu.edu.

Notes

The authors declare no competing financial interest.

ACKNOWLEDGMENTS

Dedicated to Prof. Y. Yagci on the occasion of his 60th birthday. The authors thank the CRP Consortium at Carnegie Mellon University and NSF (CHE-1026060, CHE-1039870, CHE-0130903) for financial support. K.S. thanks the Deutsche Forschungsgemeinschaft (DFG) for her postdoctoral fellowship (SCHR 1314/1-2). S.B. gratefully acknowledges support by the National Science Foundation (CHE-1055547).

REFERENCES

- (1) (a) Matyjaszewski, K.; Davis, T. P. *Handbook of Radical Polymerization*; Wiley-Interscience: Hoboken, NJ, 2002; (b) Braunecker, W. A.; Matyjaszewski, K. *Prog. Polym. Sci.* **2007**, *32*, 93–146. (c) Goto, A.; Fukuda, T. *Prog. Polym. Sci.* **2004**, *29*, 329–385. (d) Mueller, A. H. E.; Matyjaszewski, K., Eds. *Controlled and Living Polymerizations: From Mechanisms to Material*; Wiley-VCH: Weinheim, 2009. (e) Matyjaszewski, K. *J. Phys. Org. Chem.* **1995**, *8*, 197–207. (f) Matyjaszewski, K. *Macromolecules* **1993**, *26*, 1787–1788. (g) Matyjaszewski, K.; Gaynor, S.; Greszta, D.; Mardare, D.; Shigemoto, T. *J. Phys. Org. Chem.* **1995**, *8*, 306–315.
- (2) (a) Matyjaszewski, K.; Xia, J. *Chem. Rev.* **2001**, *101*, 2921–2990. (b) Wang, J.-S.; Matyjaszewski, K. *J. Am. Chem. Soc.* **1995**, *117*, 5614–5615. (c) Kato, M.; Kamigaito, M.; Sawamoto, M.; Higashimura, T. *Macromolecules* **1995**, *28*, 1721–1723. (d) Matyjaszewski, K. *Macromolecules* **2012**, *45*, 4015–4039.
- (3) di Lena, F.; Matyjaszewski, K. *Prog. Polym. Sci.* **2010**, *35*, 959–1021.
- (4) (a) Coessens, V.; Pintauer, T.; Matyjaszewski, K. *Prog. Polym. Sci.* **2001**, *26*, 337–377. (b) Gao, H.; Matyjaszewski, K. *Prog. Polym. Sci.* **2009**, *34*, 317–350. (c) Golas, P. L.; Matyjaszewski, K. *Chem. Soc. Rev.* **2010**, *39*, 1338–1354. (d) Lee, H.-i.; Pietrasik, J.; Sheiko, S. S.; Matyjaszewski, K. *Prog. Polym. Sci.* **2010**, *35*, 24–44. (e) Matyjaszewski, K.; Tsarevsky, N. V. *Nat. Chem.* **2009**, *1*, 276–288. (f) Mecerreyes, D. *Prog. Polym. Sci.* **2011**, *36*, 1629–1648. (g) Tasdelen, M. A.; Kahveci, M. U.; Yagci, Y. *Prog. Polym. Sci.* **2011**, *36*, 455–567. (h) Rikkou, M. D.; Patrickios, C. S. *Prog. Polym. Sci.* **2011**, *36*, 1079–1097. (i) Oh, J. K.; Park, J. M. *Prog. Polym. Sci.* **2011**, *36*, 168–189. (j) Zhao, Y.; Wang, L.; Xiao, A.; Yu, H. *Prog. Polym. Sci.* **2010**, *35*, 1195–1216. (k) Motornov, M.; Roiter, Y.; Tokarev, I.; Minko, S. *Prog. Polym. Sci.* **2010**, *35*, 174–211.
- (5) (a) Siegwart, D. J.; Oh, J. K.; Matyjaszewski, K. *Prog. Polym. Sci.* **2012**, *37*, 18–37. (b) McCullough, L. A.; Matyjaszewski, K. *Mol. Cryst. Liq. Cryst.* **2010**, *521*, 1–55.
- (6) Tsarevsky, N. V.; Matyjaszewski, K. *Chem. Rev.* **2007**, *107*, 2270–2299.
- (7) Matyjaszewski, K.; Jakubowski, W.; Min, K.; Tang, W.; Huang, J. Y.; Braunecker, W. A.; Tsarevsky, N. V. *Proc. Natl. Acad. Sci. U.S.A.* **2006**, *103*, 15309–15314.
- (8) (a) Jakubowski, W.; Matyjaszewski, K. *Angew. Chem., Int. Ed.* **2006**, *45*, 4482–4486. (b) Kwak, Y.; Matyjaszewski, K. *Polym. Int.* **2009**, *58*, 242–247. (c) Dong, H.; Matyjaszewski, K. *Macromolecules* **2008**, *41*, 6868–6870.
- (9) (a) Matyjaszewski, K.; Tsarevsky, N. V.; Braunecker, W. A.; Dong, H.; Huang, J.; Jakubowski, W.; Kwak, Y.; Nicolay, R.; Tang, W.; Yoon, J. A. *Macromolecules* **2007**, *40*, 7795–7806. (b) Percec, V.; Guliashvili, T.; Ladislav, J. S.; Wistrand, A.; Stjernedahl, A.; Sienkowska, M. J.; Monteiro, M. J.; Sahoo, S. *J. Am. Chem. Soc.* **2006**, *128*, 14156–14165. (c) Guliashvili, T.; Mendonca, P. V.; Serra, A. C.; Popov, A. V.; Coelho, J. F. J. *Chem.–Eur. J.* **2012**, *18*, 4607–4612. (d) Zhang, Y.; Wang, Y.; Matyjaszewski, K. *Macromolecules* **2011**, *44*, 683–685. (e) Hornby, B. D.; West, A. G.; Tom, J. C.; Waterson, C.; Harrison, S.; Perrier, S. *Macromol. Rapid Commun.* **2010**, *31*, 1276–1280. (f) Matyjaszewski, K.; Coca, S.; Gaynor, S. G.; Wei, M.; Woodworth, B. E. *Macromolecules* **1997**, *30*, 7348–7350.
- (10) Magenau, A. J. D.; Strandwitz, N. C.; Gennaro, A.; Matyjaszewski, K. *Science* **2011**, *332*, 81–84.
- (11) (a) Tinker, L. L.; McDaniel, N. D.; Bernhard, S. *J. Mater. Chem.* **2009**, *19*, 3328–3337. (b) McDaniel, N. D.; Bernhard, S. *Dalton Trans.* **2010**, *39*, 10021–10030.
- (12) (a) Tucker, J. W.; Stephenson, C. R. J. *J. Org. Chem.* **2012**, *77*, 1617–1622. (b) Yoon, T. P.; Ischay, M. A.; Du, J. *Nat. Chem.* **2010**, *2*, 527–532.
- (13) Guan, Z.; Smart, B. *Macromolecules* **2000**, *33*, 6904–6906.
- (14) (a) Tasdelen, M. A.; Uygun, M.; Yagci, Y. *Macromol. Chem. Phys.* **2010**, *211*, 2271–2275. (b) Tasdelen, M. A.; Uygun, M.; Yagci, Y. *Macromol. Rapid Commun.* **2011**, *32*, 58–62. (c) Kwak, Y.; Matyjaszewski, K. *Macromolecules* **2010**, *43*, 5180–5183. (d) Tasdelen, M. A.; Uygun, M.; Yagci, Y. *Macromol. Chem. Phys.* **2011**, *212*, 2036–2042. (e) Tasdelen, M. A.; Ciftci, M.; Yagci, Y. *Macromol. Chem. Phys.* **2012**, *213*, 1391–1396. (f) Yagci, Y.; Jockusch, S.; Turro, N. J. *Macromolecules* **2010**, *43*, 6245–6260.
- (15) (a) Fors, B. P.; Haawker, C. J. *Angew. Chem., Int. Ed.* **2012** (b) Mosnacek, J.; Ilcikova, M. t. *Macromolecules* **2012**, *45*, 5859–5865.
- (16) Bruno, T. J.; Svoronos, P. D. N. *CRC Handbook of Fundamental Spectroscopic Correlation Charts*; CRC Press, Taylor & Francis Group: Boca Raton, FL, 2006.
- (17) Schröder, K.; Mathers, R. T.; Buback, J.; Konkolewicz, D.; Magenau, A. J. D.; Matyjaszewski, K. *ACS Macro Lett.* **2012**, 1037–1040.
- (18) Sundararajan, S.; Wehry, E. L. *J. Phys. Chem.* **1972**, *76*, 1528–1536.
- (19) Tang, W.; Kwak, Y.; Braunecker, W.; Tsarevsky, N. V.; Coote, M. L.; Matyjaszewski, K. *J. Am. Chem. Soc.* **2008**, *130*, 10702–10713.
- (20) (a) David, P. G.; da Silva, P. A. C. *Bull. Chem. Soc. Jpn.* **1985**, *58*, 3566–3569. (b) Doyle, K. J.; Tran, H.; Baldoni-Olivencia, M.; Karabulut, M.; Hoggard, P. E. *Inorg. Chem.* **2008**, *47*, 7029–7034.
- (21) (a) Konkolewicz, D.; Magenau, A. J. D.; Averick, S. E.; Simakova, A.; He, H.; Matyjaszewski, K. *Macromolecules* **2012**, *45*, 4461–4468. (b) Simakova, A.; Averick, S. E.; Konkolewicz, D.; Matyjaszewski, K. *Macromolecules* **2012**, *45*, 6371–6379. (c) Bortolamei, N.; Isse, A. A.; DiMarco, V. B.; Gennaro, A.; Matyjaszewski, K. *Macromolecules* **2010**, *43*, 9257–9267.